

Hydrothermal systems on Martian crater rims: Type example at Ritchey crater and comparison to NW-Isidis crater rims.

M. C. Deahn, L. Zeng, B. Horgan *Department of Earth, Atmospheric, and Planetary Sciences, Purdue University, Indiana, USA (mdeahn@purdue.edu).*

Introduction: The approach to exploring Mars for habitability has shifted from simply "following the water" to also considering chemical reactions and energy sources [1]. A further refinement of this strategy could also include time: although habitable aqueous environments such as valley network [2] and paleolakes [3] might have existed in a warm and wet climate regime [4], impact craters could have fueled long-lived aqueous environments by their internal hydrothermal systems, regardless of climate conditions. These hydrothermal systems could have created near-surface aqueous environments with suitable temperatures to remain habitable for long periods of time throughout Mars' history. However, the history of water associated with impact-related hydrothermal systems is not yet well understood. After the collapse and modification of the transient crater [5], if target rocks are saturated with groundwater or intersected with a cryosphere, the heat released from the impact can initiate the formation of post-impact hydrothermal systems. However, it is unclear how common these environments might have been on Mars, as we currently have limited information on the nature of impact hydrothermal systems. Large impact craters are poorly preserved on Earth, and there is a general lack of remote sensing observations of possible impact-induced hydrothermal systems on Mars.

Impact-related hydrothermal systems are generated from several heat sources: (1) heat of the impact itself and (2) the melt sheet, both of which are concentrated within the crater and central peak, and (3) hot melt emplaced on the crater rim during excavation. This latter process could produce enough heat to create a long-lived low-temperature hydrothermal system in the crater rim [6,7], driving circulation of groundwater through fractures and porous breccia, which may create environments suitable for thermophilic organisms to thrive [8]. These hydrothermal systems may have produced significant alteration products on the crater rim, but more data is needed to constrain the generation and duration of hydrothermal systems, as recorded in impact crater rims, on Mars. These rim hydrothermal systems are of particular interest for orbital identification and in situ exploration because they may be better preserved over crater interior hydrothermal systems, which are rapidly buried in a hydrologically active crater basin.

There are two main challenges in utilizing remote sensing data to investigate impact-induced hydrothermal systems on Mars: 1) a large population of the ancient large impact craters have undergone significant degradation [9], including the relict hydrothermal deposits; and 2) many of the criteria used to identify impact-induced hydrothermal systems, such as specific minerals and geomorphologies, have multiple interpretations or origins. So far, only a limited number of remote sensing studies attempted to identify impact-induced hydrothermal systems on Mars (e.g., [8,10-12]). Previous mineralogical studies have largely focused on central uplift areas, but similar species of alteration minerals have also been detected in the crater wall to crater rim areas (e.g., [1,13,14]). However, the exact origins for alteration minerals at these wall-to-rim areas have remained ambiguous and have not been examined thoroughly. As such, it is unclear whether the alteration minerals formed from impact-induced hydrothermal activity, were excavated from pre-existing bedrock, or deposited by later fluvio-lacustrine processes.

We are currently evaluating a broad population of large impact craters on Mars for evidence of rim hydrothermal systems, and assessing how factors like crater size, latitude, and age affect their presence and size. Here we report (1) the clearest example of impact-driven hydrothermal alteration on a crater rim to date at Ritchey crater [7], and (2) preliminary results from a subset of our craters, in the NW circum-Isidis region. This more focused study will provide important context for the ongoing Mars 2020 exploration of the rim of Jezero crater.

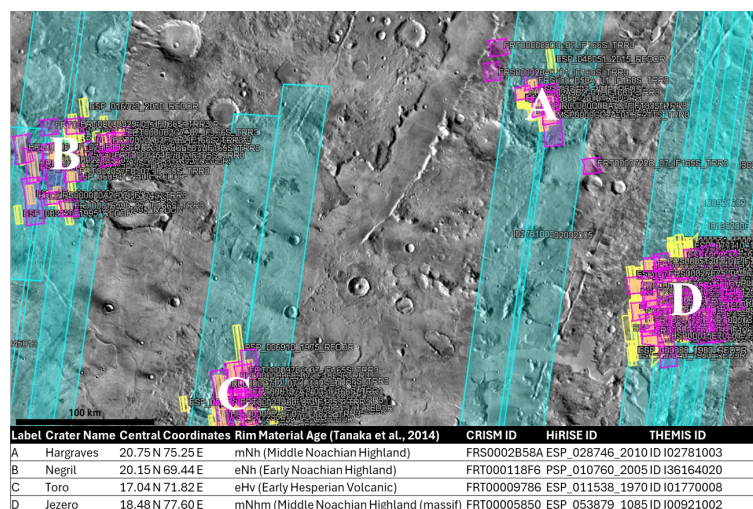


Figure 1: Four example NW-Isidis crater. Cyan, yellow, and magenta stamps are example THEMIS D875, HiRISE, and CRISM footprints respectively.

Methods: We use high-resolution orbital visible images from the High-Resolution Imaging Science Experiment (HiRISE) and hyperspectral visible/short-wave infrared (VSWIR) images from Compact Reconnaissance Imaging Spectrometer (CRISM) [15] to investigate the rims of well-preserved craters across Mars, including a suite of circum-Isidis craters (Fig. 1). We use ENVI to extract average spectra from regions of interest (ROI) along the rim, guided by CRISM spectral parameters [16]. All ROIs are ratioed to a neutral area in the same columns to help reduce signals from surface dust, residual atmospheric effects, and instrumental artifacts. The spectra are compared with diagnostic laboratory reference spectra from the USGS Spectral Library [17] and RELAB [18] databases to help with mineral identification. We include craters with a range of rim erosion states and thus exposures of a range of different materials.

Using the HiRISE and CTX basemaps, we create a catalog of morphologic expressions associated with key CRISM spectral units on each crater rim, paying special attention to features commonly associated with impact-induced hydrothermal systems, impactites, and megabreccia. For hydrothermal systems, we look for infilled fractures, mounds, and vents [8]. Impactites may appear as impact melt, which may manifest as a smooth, sheet like unit [7], perhaps with lobed shapes and cracks from cooling or tension, or even pitted textures from volatile escape [19], which may be underlain by breccia and an alteration zone due to heating by the melt [20]. Ejecta blanket typically appears as meter to decameter-scale breccia and megabreccia that consist of blocks with a variety of colors and textures [21].

We interpret possible causes of alteration in crater rims by synthesizing the spectral and geomorphic maps. Evidence of alteration below potential impactites would suggest hydrothermal systems once existed in the crater rim [7]. Alternatively, evidence of alteration minerals associated with common expressions and stratigraphies of nearby basement materials suggest uplifted and excavation of pre-existing altered

materials, and association with fluvial or lacustrine features would suggest later alteration or transport.

Type Example - Ritchey Crater: Ritchey crater is located ~200 km south of Valles Marineris and is a complex crater 78 km in diameter, with exceptionally well-preserved central uplift, terraces, rim, and ejecta [7]. The excellent preservation of Ritchey crater offers a unique opportunity to study impactite-alteration stratigraphy on the rim for large, complex craters on Mars.

Stratigraphic sequence: On the inner rim of Ritchey crater, the most common stratigraphic sequence presents as fractured light-toned bedrock overlain by a fragmented breccia unit and capped by a darker-toned sheet-like unit [7]. Outcrops of light-toned massive bedrock at the base of the sequence exhibit a ridged texture, with smooth escarpments along their slope. On the top, the sheet unit forms a ten- to decameters-thick coherent layer that can be traced laterally across several km.

Spectral properties: CRISM spectra of typical basement rocks in the Ritchey crater rim show strong pyroxene absorption bands (0.9–1.0 μm , 1.9–2.0 μm) most consistent with low-Ca pyroxene (LCP), with no associated alteration mineral detections [14]. The sheet-like unit also shows broad absorptions centered near 0.9 and 1.9 μm consistent with LCP, but with a shoulder near 1.2 μm potentially due to mixing with olivine or glass, [22] and appears to be unaltered. In contrast, the fragmented breccia does not show pyroxene bands and instead resembles olivine or glass with a broad band centered $>1.0 \mu\text{m}$, and a weak possible band at 1.9 μm , suggesting minimal hydration. In contrast, strong signatures of alteration are detected in the ridged unit and altered bedrock underlying the breccia. A clear 2.29–2.31 μm band and weak 1.39–1.42 μm band in the ridged unit suggest the presence of Fe/Mg-bearing phyllosilicates such as nontronite and saponite. Many outcrops also show evidence for Mg-carbonate based on an additional 2.51–2.53 μm band and 3.4–3.5 μm band, 3.9 μm band drop related to CO₂ overtones and combinations [7].

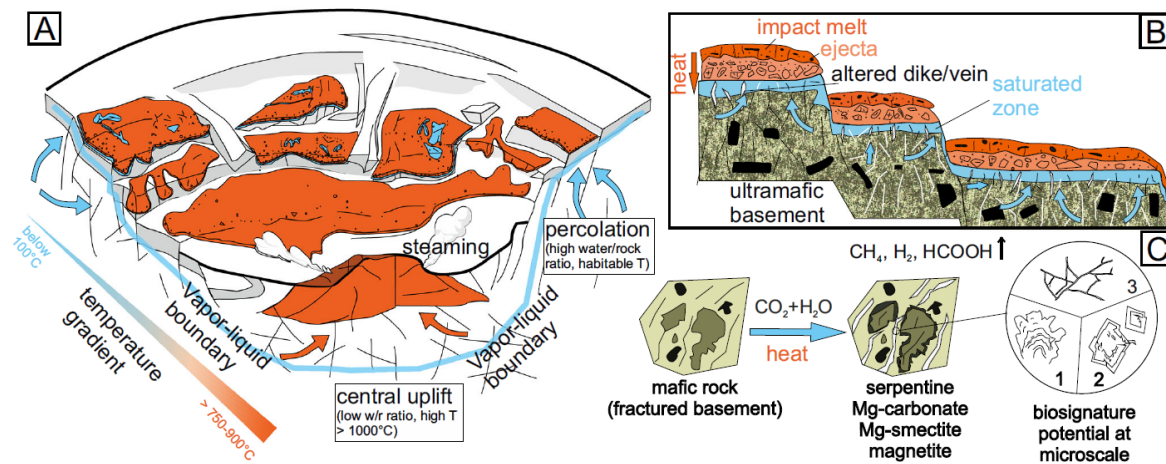


Figure 2: Schematic model of early post impact phase with active groundwater hydrothermal percolation (A and B) and alteration processes at the microscale (C) from Zeng and Horgan (2025) [7].

Proposed model of Ritchey crater hydrothermal system: We hypothesize that the diverse alteration minerals in the Ritchey crater rim track the evolution of the aqueous system following the cooling of the impact melt (Fig. 2). Impact melt glass forms at a temperature higher than 1870 °C [23]. During the emplacement of the melt sheet on the rim area, the incorporation of cooler in situ fragmented materials into the melt-rich breccia leads to a lower temperature of >750–900 °C compared to the central peak and basin-filling melt sheet [10,20,24]. The emplaced melt is thicker in the crater basin than on the wall to-rim area and thus maintain a hot crater floor over time. Furthermore, uplifted, hot materials at the central peak provide additional heat to the area.

Together, these effects result in a decreasing gradient in temperature [10,25] and alteration strength [26] from crater center to crater rim. As the melt is cooling down, hydrothermal alteration would have driven a series of low-temperature alteration reactions below 400 °C: (1) Chlorite-related alteration commonly between 300 to 400 °C (e.g., chlorite-bearing assemblage at Sudbury impact structure on Earth [27]); (2) Serpentinization (<150 to 400 °C), one of the most important reactions for astrobiological interests because it mobilizes critical elements and delivers chemicals (such as hydrogen and methane) to support critical microbial metabolism similar to the earliest biogeochemical cycles on Earth [28]; (3) low temperature (<100 °C) carbonation to form saponite and carbonate [29].

Hydrothermal modeling of a complex crater comparable to Ritchey predicts that the hydrothermal alteration below 200 °C occurs on the crater rim for at least 20,000 years [25]. Low temperature hydrothermal sites at crater rims (Fig. 2) could have provided potential habitable environment outside the central peaks, where most hydrothermal fluids were suggested to emerge previously [8,11,12,30]. Minerals like hydrated silica and carbonate precipitated from hydrothermal fluids could preserve biosignatures from these environments [31] (Fig. 2).

NW-Isidis Investigation: The Mars 2020 Perseverance rover is exploring and collecting samples from the rim of Jezero, another large Noachian crater on Mars that likely also produced hydrothermal systems. For sampling, crater rims would be more accessible than any preserved central peak materials, if they exist, within the crater. Rock samples from impact hydrothermal deposits would be a high priority as they could have high biosignature preservation potential [32]. In our study, we aim to build a catalog of complex crater alteration minerals present in Jezero-like NW-Isidis crater rims (Fig. 2) following the model proposed at Ritchey crater [7].

Based on orbital data, previous studies pointed out that the smectite and carbonate detected on and within the rim of Jezero crater could be authigenic precipitation or alteration products from various processes, including fluvial, lacustrine, or low-temperature

hydrothermal activity [33]. These alteration minerals could have preserved geochemical information of the former habitable environment and were proposed as targets for Mars 2020 sample return mission [34,35]. While the origin of alteration minerals in the rim can be assessed by the Perseverance rover, interpreting these in situ results will still be challenging without a clear framework for the mineralogical, textural, and stratigraphic properties of impact hydrothermal systems more generally.

In addition to Jezero, the northwestern circum-Isidis region hosts other more recent and less eroded impact craters with well exposed internal structures and ejecta deposits (i.e. Hargraves Crater) [19], and that may have hosted impact-induced hydrothermal systems (i.e. Toro Crater) [1]. The objective of this research is to constrain the origin of alteration materials in the rims of NW-Isidis craters by creating a framework of possible impact crater rim hydrothermal systems on Mars.

Preliminary Study at Toro Crater: Toro crater is a well preserved, ~ 40 km complex crater located on the western edge of the Isidis basin in the northern region of the Syrtis Major Volcanic Plains (SMVP) [8] (Fig. 1C). The crater is characterized by its sharp rim, terraced crater walls, and high (~ 400 m above the floor) central peak. Morphologic features including light-toned fractures on the crater floor, and putative hydrothermal mounds in the central uplift are suggested to be evidence of hydrothermal activity [8]. These mounds are also found in other impact craters on Mars associated with hydrothermal systems [10].

Previous studies focus primarily on Toro crater's central uplift and conclude that the hydrothermal activity cannot be attributed to only excavation of altered subsurface materials or impact-induced hydrothermal alteration [8]. Our preliminary look at Toro crater aims to address the question: does Toro crater's rim preserve mineralogical evidence of impact-induced hydrothermal systems on Mars?

Compositional maps of Toro crater rim. Three primary mafic minerals are identified on the Toro crater rim. Olivine is dominantly found at the base of the rim, and has characteristic absorption features at 0.84, 1.05, and 1.25 μm [16]. High-calcium pyroxene is found in the rim wall distinguished by broad absorption features from 0.95 – 1.02 μm and 2.05 – 2.2 μm . Low-calcium pyroxene is characterized by its shorter wavelength absorption features, at 0.90 – 0.95 μm and 1.9 – 2.05 μm and is primarily found in large quantities at the top of the rim.

Phyllosilicates including prehnite, chlorite, nontronite, and saponite are seen in the rim (Fig. 3). Prehnite is distinguishable from chlorite by a characteristic 1.48 μm absorption feature. Nontronite and saponite have 1.4, 1.9, and 2.3 μm absorption features, that are shifted depending on the Fe or Mg content [16]. The spectral features measured in the rim fall somewhere in between, which suggests a mix of

both smectites. Al phyllosilicates are also found within the rim (Fig. 3). Montmorillonite has 1.4, 1.9, and a characteristic 2.2 μm absorption feature [16]. Opal or hydrated silica exhibits similar absorptions, but the 2.2 μm feature tends to be broader [8].

Geomorphic features in Toro crater rim. Morphologic features commonly associated with impact-induced hydrothermal systems include mounds, vents, and fractures [8]. High-resolution images of the Toro crater rim reveal meter-scale rim-parallel fractures. Also found along the rim in small clusters are what appear to be mounds of light-toned materials with dark aprons, which match previous descriptions of putative hydrothermal mounds found in the central uplift of Toro crater [8].

Discussion: Did Toro host an impact-induced hydrothermal system? The alteration minerals on the rim of Toro crater may have been produced by impact-induced hydrothermal alteration. Spectroscopic evidence of minerals indicative of high and low temperature hydrothermal alteration (prehnite and Fe/Mg smectites, respectively) are found within the study region. The presence of significant amounts of prehnite suggests the materials in the rim were at one point exposed to metamorphic conditions of low, <3 kbar pressure and high temperatures between 200–350°C, that are consistent with the high temperature created by the shock of an impact event [36]. The presence of lower temperature hydrated minerals and Al phyllosilicates also supports a waning hydrothermal system over time (the aftereffects of an impact large enough to create a complex crater).

Evidence of morphologic features consistent with hydrothermal activity on the rim (i.e. fractures and vents) [8,11] also support the impact-induced hydrothermal system hypothesis. These mounds and light-toned fractures may be the source of some of the altered hydrated minerals as they are more consistent with morphologies seen post-impact. Similar features are found in the central uplift of Toro crater, but they alone cannot discount the uplift and excavation hypothesis for some of the altered minerals in Toro crater [8].

Future work. While our preliminary look at Toro crater summarizes the types of minerals that may be present in the crater rim, further work needs to be done to constrain their placement in the rim stratigraphy. According to previous analyses of Ritchey crater, a key test of an impact hydrothermal origin is close association with impactite materials and potential impact melt. If Toro crater hosted an impact-induced hydrothermal system, we would expect to find a diverse

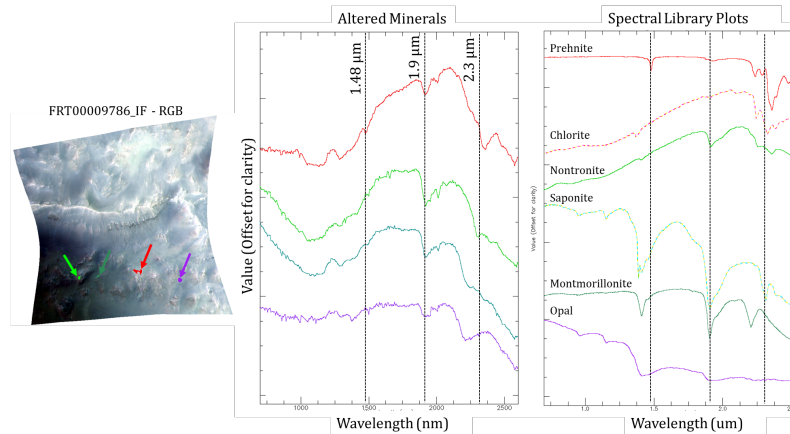


Figure 3. Measured Fe/Mg and Al phyllosilicate spectra and USGS Spectral Library and RELAB database spectra for phyllosilicates [35,36].

array of impactite-alteration minerals within the local rim stratigraphy. We would then repeat this analysis for other NW-Isidis crater rims including Jezero crater, which may help inform future sample return targets on Jezero’s rim.

References: [1] Amador et al. (2018), *Icar.*, 311, 113-134. [2] Fassett et al. (2008), *Icar.*, 198, 37-56. [3] Goudge et al. (2015), *Icar.*, 260, 346-367. [4] Craddock et al. (2002), *JGRP*, 107, 21-1-21-36. [5] Melosh (1989) *Oxford Univ. Press*. [6] Ivanov et al. (2011), *Meteorit. Plan. Sci.* 46, 601–619. [7] Zeng & Horgan (2025), *Nat. Comm.*, 16, 3240. [8] Marzo et al. (2010), *Icar.*, 208, 667–683. [9] Robbins and Hynek (2012), *JGRP*, 117, E5. [10] Osinski et al. (2013), *Icar.*, 224, 347-363. [11] Turner et al. (2016), *JGRP*, 121, 608-625. [12] Carrozzo et al. (2017), *Icar.*, 281, 228-239. [13] Ehlmann et al. (2010) *JGR*, 37. [14] Sun & Milliken (2014), *JGRP*, 119, 810-836. [15] Murchie et al. (2007), *JGRP*, 112. [16] Viviano et al. (2014), *JGRP*, 119, 1403-1431. [17] Kokaly et al. (2017), *USGS Spect. Lib.* v. 7. [18] Milliken, (2020) *NASA Reflec. Exp. Lab. Spect. Lib* [19] Sacks L. E. et al. (2022), *Icar.*, 375, 114854. [20] Osinski et al. (2011), *EPSL*, 310, 167-181. [21] Scheller & Ehlmann (2020), *JGRP*, 125, e2019JE006190. [22] Cannon & Mustard (2015), *Geol.*, 43, 635-638. [23] El Goresy (1965), *JGR*, 70, 3453-3456. [24] Englehardt et al. (1995), *Meteorit.*, 30, 279-293. [25] Abramov & Kring (2005), *JGRP*, 110. [26] Schwenzer & Kring (2013), *Icar.*, 226, 487-496. [27] Molnar et al. (2001), *Econ. Geol.* 96, 1645-1670. [28] Russell et al. (2010), *Geobio.*, 8, 355-371. [29] Kelemen & Hirth (2012), *EPSL*, 345-348, 81-89. [30] Sun & Milliken (2015), *JGRP*, 120, 2293-2332. [31] Hays et al. (2017), *Astroble.*, 17, 363-400. [32] Beaty et al. (2019), *Meteorit. Plan. Sci.*, 54, S3-S152. [33] Horgan et al. (2020), *Icar.*, 339, 113526. [34] Gupta & Horgan (2018), *Mars2020 4th LSW*. [35] Farley et al. (2020), *Space Sci. Rev.*, 216, 142. [36] Ehlmann et al. (2009), *JGRP*, 114, E2.